Whytock, KL, Parry, SA, Turner, MC, Woods, RM, James, LJ, Ferguson, RA, Ståhlman, M, Borén, J, Strauss, JA, Cocks, MS, Wagenmakers, AJM, Hulston, CJ and Shepherd, SO

A 7-day high-fat, high-calorie diet induces fibre-specific increases in intramuscular triglyceride and perilipin protein expression in human skeletal muscle

Whytock, KL, Parry, SA, Turner, MC, Woods, RM, James, LJ, Ferguson, RA, Ståhlman, M, Borén, J, Strauss, JA, Cocks, M, Wagenmakers, AJM, Hulston, CJ and Shepherd, SO

A high-fat high-calorie diet induces fibre-specific increases in intramuscular triglyceride and perilipin protein expression in human skeletal muscle.

A high-fat high-calorie diet induces fibre-specific increases in intramuscular triglyceride and perilipin protein expression in human skeletal muscle

Whytock KL[1], Parry SA[2], Turner MC[2], Woods RM[2], James LJ[2], Ferguson RA[2], Ståhlman M[3], Borén J[3], Strauss JA[1], Cocks M[1], Wagenmakers AJM[1], Hulston CJ[2] & Shepherd SO[1]

1) Research Institute of Sport and Exercise Science, Tom Reilly Building, LJMU, Liverpool, UK, L3 3AF
2) School of Sport, Exercise and Health Sciences, Loughborough University, Loughborough, Leicestershire, LE11 3TU
3) Wallenberg Laboratory, Sahlgrenska Academy, University of Gothenburg, Gothenburg, Sweden

Corresponding author: Sam O Shepherd, S.Shepherd@ljmu.ac.uk

Running title: HFHC diet increases IMTG and PLINs

Key words: high-fat, intramuscular triglyceride, perilipin, confocal immunohistochemistry

Key points:

- We have recently shown that a high-fat high-calorie (HFHC) diet decreases whole body glucose clearance without impairing skeletal muscle insulin signalling, in healthy lean individuals.
- These diets are also known to increase skeletal muscle IMTG stores, but the effect on lipid metabolites leading to skeletal muscle insulin resistance has not been investigated.
- This study measured the effect of 7 days HFHC diet on: 1) skeletal muscle concentration of lipid metabolites, and 2) potential changes in the perilipin (PLIN) content of the lipid droplets (LD) storing IMTG.
- The HFHC diet increased PLIN3 protein expression and redistributed PLIN2 ~~into~~ to LD stores in type I fibres.
- The HFHC diet increased IMTG content in type I fibres, while lipid metabolite concentrations remained the same. The data suggest that the increases in IMTG stores assists reducing the accumulation of lipid metabolites known to contribute to skeletal muscle insulin resistance.

Abstract

A HFHC diet reduces whole body glucose clearance without impairing skeletal muscle insulin signalling in healthy lean individuals. HFHC diets also increase skeletal muscle lipid stores. However, unlike certain lipid metabolites, intramuscular triglyceride (IMTG) stored within lipid droplets (LD) does not directly contribute to skeletal muscle insulin resistance. Increased expression of perilipin (PLIN) proteins and colocalisation to LD has been shown to assist in IMTG storage. We aimed to test the hypothesis that 7 days on a HFHC diet increases IMTG content while minimising accumulation of lipid metabolites known to disrupt skeletal muscle insulin signalling in sedentary and obese individuals. We also aimed to identify changes in expression and subcellular distribution of proteins involved in IMTG storage. Muscle biopsies were obtained from the *m. vastus lateralis* of 13 (n = 11 males, n = 2 females) healthy lean individuals (age: 23±2.5 y, BMI: 24.5±2.4 kg.m^{-2}), following an overnight fast, before and after consuming a high-fat (64% energy) high-calorie (+47% kcal) diet for 7 days. After the HFHC diet, IMTG content increased in type I fibres only (+101%; P<0.001), whereas there was no change in the concentration of either total diacylglycerol (P=0.123) or total ceramides (P=0.150). Of the PLINs investigated, only PLIN3 content increased (+50%; P<0.01) solely in type I fibres. LDs labelled with PLIN2 increased (80%; P<0.01), also in type I fibres only. We propose that these adaptations to LD support IMTG storage and minimise accumulation of lipid metabolites to protect skeletal muscle insulin signalling following 7 days HFHC diet.

Introduction

Peripheral insulin resistance is a prominent feature of the type 2 diabetic phenotype (DeFronzo & Tripathy, 2009). Skeletal muscle serves as one of the largest depots for insulin-stimulated glucose uptake (Katz *et al.*, 1983; Ferrannini *et al.*, 1985), and impairments in skeletal muscle insulin sensitivity are therefore a contributing factor to peripheral insulin resistance and ensuing hyperglycaemia. Elevated intramuscular triglyceride (IMTG) stores are associated with insulin resistance in sedentary, obese and/or type 2 diabetes individuals (Kelley *et al.*, 1999; Goodpaster *et al.*, 2001), but this association is not seen in endurance trained individuals as they are able to combine large IMTG stores with very high insulin sensitivity. This phenomenon is known as 'the athlete's paradox' (Goodpaster *et al.*, 2001; van Loon *et al.*, 2004). To understand the relationship between IMTG content and skeletal muscle insulin resistance, previous studies have used intravenous lipid/heparin infusions in order to mimic the elevated plasma fatty acid and triglyceride (TAG) supply to skeletal muscle, a characteristic of the obese and type 2 diabetic phenotype (Boden *et al.*, 1994; Itani *et al.*, 2002; Yu *et al.*, 2002; Szendroedi *et al.*, 2014). From these studies it has become apparent that IMTG *per se* is not mechanistically linked to impaired skeletal muscle insulin signalling. Rather, accumulation of lipid metabolites in skeletal muscle, such as diacylglycerols (DAGs) and ceramides, have been implicated in skeletal muscle insulin resistance. The relationship between DAGs and insulin resistance remains controversial however, since they are elevated in insulin-sensitive endurance-trained athletes (Amati *et al.*, 2011). Previous research has shown that these lipid metabolites directly interfere with components of the insulin signalling cascade and lead to reductions in insulin-stimulated glucose uptake (Itani *et al.*, 2002; Yu *et al.*, 2002; Szendroedi *et al.*, 2014).

High-fat, high-calorie (HFHC) diets provide an experimental model of lipid excess that are more physiologically relevant than that of lipid infusion protocols, as they match the dietary

habits of the 'Western world'. We, and others, have consistently shown that short-term (3-7 days) adherence to a HFHC diet can reduce insulin sensitivity and glycaemic control in healthy individuals (Bakker *et al.*, 2014; Hulston *et al.*, 2015; Gemmink *et al.*, 2017; Parry *et al.*, 2017). Importantly, it was recently reported that 3 days of excessive dietary fat intake reduced insulin-stimulated leg glucose uptake without changes in skeletal muscle signalling (Lundsgaard *et al.*, 2017). This is very similar to our own observations, where 7 days on a HFHC diet resulted in reduced postprandial glycaemic control that was attributable to reduced glucose clearance (determined using dual-glucose tracers during an oral glucose challenge) despite maintained skeletal muscle insulin signalling (Parry *et al.*, 2019). Based on this observation, we hypothesise that the lipid metabolites known to lead to skeletal muscle insulin resistance in sedentary, obese and type 2 diabetes individuals are not elevated when healthy lean individuals consume a 7-days HFHC diet and that most of the diet-derived fatty acids (FA) will be stored as IMTG instead.

IMTG is stored within lipid droplets (LD) which are coated by a phospholipid monolayer, decorated with numerous proteins (Bersuker & Olzmann, 2017). The most extensively studied of these proteins is the perilipin (PLIN) family of proteins. Increases in the protein expression of PLIN2 and/or PLIN5 occur alongside elevations in IMTG content induced by exercise training (Shaw *et al.*, 2012; Shepherd *et al.*, 2013; Shepherd *et al.*, 2014) or a HFHC diet (Gemmink *et al.*, 2017), indicating that the PLIN proteins play a role in IMTG storage. In support, myotubes overexpressing PLIN3 accumulate IMTG (Kleinert *et al.*, 2016), and PLIN5 overexpression in primary human myotubes or rat skeletal muscle augments IMTG content whilst restricting accumulation of lipid metabolites (DAGs or ceramides) concomitant to preserved insulin sensitivity (Bosma *et al.*, 2013; Laurens *et al.*, 2016). Not only is the protein expression of the PLIN proteins important, but also their distribution across LDs. We have previously shown that LDs with PLIN attached are targeted for

breakdown during exercise (Shepherd *et al.*, 2012, 2013). Moreover, reductions in insulin sensitivity in response to prolonged fasting are least severe in those individuals who can redistribute PLIN5 across an expanded LD pool (Gemmink *et al.*, 2016). This suggests that increasing the number of LDs with PLIN proteins on the LD surface may help to alleviate lipid-induced insulin resistance. This mechanism may explain the observation recently made by our group (Parry *et al.*, 2019) that skeletal muscle insulin signalling is maintained following 7 days on a HFHC diet.

The primary aim of this study was to test the hypothesis that in healthy individuals that have consumed a HFHC diet for 7 days there is an increase in IMTG stores and a reduction or no change in the concentration of lipid metabolites known to disrupt the insulin signalling cascade in insulin resistant states. Fibre type and subcellular distribution of IMTG, as well as the size of LD containing IMTG are all closely linked to insulin resistance (Chee *et al.*, 2016; Nielsen *et al.*, 2017; Daemen *et al.*, 2018). To detect nuanced changes in IMTG stores following a HFHC diet we employed our previously validated microscopy techniques (Shepherd *et al.*, 2012, 2013; Shepherd *et al.*, 2017) to allow us to investigate changes in LD morphology and subcellular distribution on a fibre type-specific basis. PLIN proteins have been implicated in IMTG storage and therefore we also hypothesised that there would be an increase in PLIN protein content and PLIN colocalisation to LD following the HFHC diet.

Methods

Participants and ethical approval

The samples used in this study were collected as part of a previous study investigating the effect of 7 days HFHC diet on glucose kinetics and insulin sensitivity (Parry *et al.*, 2019). Muscle samples from 13 healthy individuals (*n* = 11 males and *n* = 2 females, (age: 23±1 y, BMI: 24.5±0.7 $kg.m^{-2}$) were used for the analysis of this study, with the informed consent provided originally covering this subsequent use. All participants were physically active (taking part in at least 3 x 30 min of moderate-intensity physical activity each week), non-smokers, with no diagnosis of cardiovascular or metabolic disease, not taking any medication known to interfere with the study outcomes, and weight stable for at least 3 months. The study adhered to the Declaration of Helsinki and was approved (R13-P171) by Loughborough University Subcommittee Ethical Committee for Human Participants. All participants provided written informed consent. The study was registered at ClinicalTrials.gov (identifier: NCT03879187).

Pre-testing

Prior to the start of the study, participants attended the laboratory for an initial assessment of their baseline anthropometric characteristics (height, body mass and BMI). This information was then used to estimate resting energy expenditure (REE) (Mifflin *et al.*, 1990). A standard correction for physical activity (1.6 and 1.7 times REE for females and males, respectively) was applied in order to estimate total daily energy requirements. This information was then used to determine individual energy intakes for the experimental diet intervention (Parry *et al.*, 2017).

Experimental protocol

Participants consumed a high-fat (64% energy), high-calorie (+47% kcal) (HFHC) diet for 7 days. The diet provided 4646 ± 194 kcal per day, with 185 ± 9 g [16% total energy (TE)] protein, 233 ± 9 g [20% TE] carbohydrate, and 325 ± 15 g [64% TE] fat intake. Saturated fat intake was 140 ± 6 g [27.5% TE]. All foods were purchased and prepared by the research team. Participants were instructed to eat everything that was provided, not to eat any additional food, and to return any uneaten items so that diet values could be adjusted if necessary. All participants were informed about the importance of strict diet adherence. Adherence was checked by daily interviews that were conducted when participants collected their food bundles. Muscle biopsies were performed before and after the HFHC diet. Biopsies were performed after an overnight fast (>12 h), having refrained from strenuous physical activity for ≥ 48 h. Samples were obtained from the *m. vastus lateralis* under local anaesthesia using the Bergstrom needle biopsy technique with suction (Bergström, 1975). Following removal of excess blood, fat and connective tissue, a portion of muscle (10-30 mg) was mounted in Tissue-Tek OCT (Sakura Finetek UK Ltd) and frozen in liquid nitrogen-cooled isopentane for subsequent immunohistochemical analyses. Another portion of muscle tissue (20-30 mg) was freeze-dried, dissected and cleaned for biochemical lipid metabolite analysis.

Lipid composition analysis

Approximately 5 mg of freeze-dried muscle tissue (20-30 mg wet weight) was used for the lipid composition analysis using the butanol:methanol [3:1] (BUME) method (Lofgren *et al.*, 2016). Briefly BUME solution was added to samples at -20^{o}C and combined tissue homogenization and lipid extraction were then performed using a Mixer Mill 301 instrument (Retsch GmbH, Haan, Germany). Automated liquid handling steps in the extraction procedure were performed by a Velocity 11 Bravo pipetting robot (Agilent technologies,

Santa Clara, CA, USA). Total lipid extracts were stored in chloroform/methanol (2:1) at -20^{o}C until further analysis. Prior to mass spectrometric analysis DAG was fractionated using straight-phase high-performance liquid-chromatography (HPLC) and ELS detection as previously described (17). For mass spectrometric analysis, total lipid extracts, as well as the DAG fractions, were diluted with internal standard-containing chloroform/methanol (1:2) with 5mM ammonium acetate. TAG and DAG were then quantified by direct infusion (shotgun) on a QTRAP 5500 mass spectrometer (Sciex, Concord, Canada) equipped with a robotic nanoflow ion source, TriVersa NanoMate (Advion BioSciences, Ithaca, NJ) performed in positive ion mode by neutral loss detection of 10 common acyl fragments formed during collision induced dissociation, according to previous work (Murphy *et al.*, 2007). Lipid class-specific internal standards were used of either deuterated or diheptadecanoyl (C17:0) containing fatty acids.

Ceramides were analysed using UPLC-MS/MS according to previous work (Amrutkar *et al.*, 2015). Prior to ceramide analysis the total extract was exposed to alkaline hydrolysis (0.1M potassium hydroxide in methanol) to remove phospholipids that could potentially cause ion suppression effects. After hydrolysis the samples were reconstituted in chloroform:methanol:water [3:6:2]. Ceramides were then quantified using a QTRAP 5500 mass spectrometer equipped with an Infinity quaternary ultra-performance pump (Agilent Technologies, Santa Clara, CA).

Immunohistochemistry analysis

Serial cryosections (5 μm) were cut at -30^{o}C onto ethanol-cleaned glass slides. Cryosections of samples obtained pre and post 7 days HFHC diet from one participant were placed on a single slide to account for any variation in staining intensity between sections. Sections were fixed for 1 h in 3.7% formaldehyde, rinsed 3 x 30 s in doubly distilled water (dd H_2O) and permeabilised in 0.5% Triton X-100 for 5 min, before being washed 3 x 5 min in Phosphate

196 Buffered Saline (PBS, 137mM sodium chloride, 3 mM potassium chloride, 8 mM sodium
197 phosphate dibasic and 3mM potassium phosphate monobasic, pH of 7.4). Slides were
198 incubated for 1 h with primary antibodies, washed 3 x 5 min in PBS, incubated with
199 complementary secondary fluorescence-conjugated antibodies for 30 min, followed by a
200 further 3 x 5 min PBS washes. To visualise IMTG, LD were incubated for 20 min with the
201 free fluorochrome BODIPY 493/503 (Invitrogen, Paisley, UK, D3922), which due to its
202 lipophobic nature partitions into the core of LDs. Following a single 5 min PBS wash,
203 coverslips were mounted with Vectashield (H-1000, Vector Laboratories, Burlingame, CA,
204 USA) and sealed with nail varnish.

205 *Antibodies and staining combinations*

206 The primary antibodies used were guinea pig anti-adipophilin (PLIN2) and guinea pig anti-
207 OXPAT (PLIN5: both Progen, GP40 & GP31 respectively, Biotechnik, Heidelberg,
208 Germany), rabbit anti-perilipin 3/TIP-47 (PLIN3: NB110-40764 Novus Biologicals,
209 Cambridge, UK), mouse anti-OxPhos Complex IV subunit I (COXIV; used as a marker of
210 muscle oxidative capacity: 459600, ThermoFisher Scientific, Paisley, UK), mouse anti-
211 dystrophin (used as a plasma membrane marker: D8168, Sigma-Aldrich, Dorset UK). Cell
212 border visualisation was achieved with either rabbit anti-laminin (L9393, Sigma-Aldrich,
213 Dorset, UK) or with wheat germ agglutinin (WGA) Alexa Fluor 633 conjugate
214 (ThermoFisher Scientific, Paisley, UK). Muscle fibre type was determined using mouse anti-
215 myosin heavy chain I (MHCI) (A4.840c) and mouse anti-myosin heavy chain IIa (MHCIIa)
216 (N2.261c; both DSHB, University of Iowa, USA developed by Dr. Blau). Appropriate Alexa
217 Fluor secondary antibodies were obtained from ThermoFisher Scientific (Paisley, UK).

218 To determine fibre type-specific protein expression, primary antibodies targeting PLIN2,
219 PLIN3, PLIN5 or COXIV, or BODIPY 493/503 to stain for IMTG, were used in combination
220 with antibodies targeting fibre type (MHCI, MHCIIa) and the cell border (either laminin or

WGA Alexa Fluor 633 conjugate). To investigate colocalisation between PLIN proteins and LD, PLIN2, PLIN3 or PLIN5 were stained in combination with BODIPY 493/503, and antibodies targeting fibre type (MHCI and MHCIIa).

Image capture, processing and data analysis

All images were captured using an inverted confocal microscope (Zeiss LSM710; Carl Zeiss AG, Oberkochen, Germany) with a 63x 1.4 NA oil immersion objective. A diode laser was used to excite the Alexa Fluor 405 fluorophore, an argon laser for the Alexa Fluor 488 fluorophore and BODIPY 493/503 and a helium-neon laser for the Alexa Fluor 546 and 633 fluorophores.

To assess IMTG content, and the protein expression of the PLIN proteins and COXIV cross-sectional images were obtained at 1.1x digital zoom. Type I and type IIa fibres were identified through positive staining, and any fibres without positive staining for either MHCI or MHCIIa were assumed to be type IIx fibres. For type I and IIa fibres 10 images per fibre-type per participant pre and post the HFHC diet for each assay was obtained (equating to a total of 260 images per assay). This was not possible for type IIx fibres due to a low number of these fibres in muscle sections in a number of participants. Type IIx fibres were included in the analyses if it was possible to obtain 4 or more images of type IIx fibres per time point for a participant. This equated to an average of 71 ± 11 images of type IIx fibres being used in the 5 assays that we were able to acquire a sufficient quantity of type IIx fibres to be used in statistical analyses. Image analysis was undertaken using Image-Pro Plus, version 5.1 (Media Cybernetics, Bethesda, MD, USA). To assess IMTG and PLIN protein content within each muscle fibre, the fibre was first separated into a peripheral region (first 5 μm from the cell border) and the central region (remainder of the cell; Figure 1). A selected intensity threshold was used to represent a positive signal for IMTG and each PLIN protein. IMTG and PLIN protein content was expressed as the positively stained area fraction relative to the total

area of the peripheral region or central region of each muscle fibre. Data was also extracted to examine LD number (number of LDs expressed relative to area) and LD size (mean area of individual LDs). COXIV fluorescence intensity was calculated using optical density in the peripheral and central regions of the cell and normalised to each individual peripheral and central area.

As previously described (Shepherd *et al.*, 2013; Strauss *et al.*, 2016; Whytock *et al.*, 2018), before any colocalisation analysis was undertaken controls were included to confirm absence of 1) bleed through of fluorophores in opposing channels when single staining was performed, 2) non-specific secondary antibody binding, and 3) sample autofluorescence. For colocalisation analysis of PLIN proteins with LD, images were obtained at 4x digital zoom applied to both the centre region and the peripheral region of type I and type IIa muscle fibres pre and post the HFHC diet (n=10 images per region, per fibre-type, pre and post HFHC diet, per participant, equating to a total of 80 images for each participant for each staining protocol; Figure 2). Object-based colocalisation analysis was performed separately for PLIN2, PLIN3 and PLIN5 with LD, as previously described (Shepherd *et al.*, 2012, 2013; Shepherd *et al.*, 2017). Briefly, a selected intensity threshold was used to denote a positive signal for each PLIN protein of interest and LD. These thresholds were used to produce binary images of the PLIN protein and LD used for the colocalisation analysis (Figure 2B and C). Binary images were merged to produce a colocalisation map and overlapping regions extracted to a separate image (Figure 2D and E). The number of extracted objects was calculated and expressed relative to area to represent the number of PLIN-associated LD (PLIN+ LD). The number of extracted objects was subtracted from the total number of LD and expressed relative to area to represent the number of LD not associated with PLIN (PLIN- LD). Additionally, the number of extracted objects was subtracted from the total number of PLIN objects and expressed relative to area to identify the amount of free PLIN

protein not associated with LD. The fraction of PLIN protein colocalising to LD was also reported. When conducting the colocalisation analysis, if there were multiple PLIN objects localised to a single LD this was classified as one colocalisation count, in order to avoid over estimation of PLIN+ LD.

Statistics

All data is reported as the mean ± SD, including the figures. Significance was set at $P < 0.05$. A paired t-test was used to compare overall results from pre to post HFHC diet. A linear mixed-effects model with fixed effects for fibre-type (type I vs type IIa vs type IIx), region (central vs peripheral) and time (pre vs post HFHC diet) and random effects to account for repeated measurements within subjects was used. Significant main effects or interaction effects were assessed using Bonferroni adjustment *post hoc* analysis.

Results

Lipid metabolites

Total TAG did not change from pre (22.53 ± 30.32 nmol/mg tissue) to post the HFHC diet (11.91 ± 15.02 nmol/mg tissue; $P = 0.34$; Figure 3A). From pre to post HFHC diet there was also no changes in total DAG content (1.63 ± 1.85 and 0.67 ± 0.84 nmol/mg tissue pre and post HFHC diet respectively; $P = 0.123$; Figure 3B) or total ceramide content (169.30 ± 194.54 and 74.42 ± 7.48 pmol/mg tissue pre and post HFHC diet respectively; $P = 0.150$; Figure 3C). Individual species of DAG (Figure 3D) and ceramides (Figure 3E) also showed no changes from pre to post HFHC diet.

IMTG analysis

At baseline, type I fibres had greater IMTG content (expressed as percentage of fibre stained) in comparison to type IIa ($P = 0.006$) and type IIx fibres ($P < 0.001$), although there was no difference between type IIa and type IIx fibres ($P = 0.467$; Figure 4A). There was also no

significant differences in IMTG content at baseline between the peripheral and central region of the cell ($P = 0.399$). Following the HFHC diet there was an increase in IMTG content that was exclusive to type I fibres only (+101%; $P < 0.001$), and this occurred in both the peripheral (+89%; $P < 0.001$) and central regions (+103; $P < 0.001$). Although overall IMTG content did not increase in type IIa or IIx fibres, IMTG content did increase in the peripheral region of both fibres following the HFHC diet (type IIa fibres +117%; $P = 0.016$; and type IIx fibres +134%; $P = 0.016$). Consequently, following the HFHC diet IMTG content was greater in the peripheral region of muscle fibres compared to the central region ($P = 0.022$).

The increase in IMTG content in type I fibres was due to an increase in both LD size (+44%; $P < 0.001$; Figure 4B) and LD number (+43%; $P < 0.001$; Figure 4C) in both muscle fibre regions. Although overall IMTG content was not augmented by HFHC diet in type IIa and type IIx fibres, we did observe an increase in LD size in both the peripheral (+36% and +30% for type IIa and IIx respectively; $P < 0.01$) and central region (+47% and +46% for type IIa and IIx fibres respectively; $P < 0.001$) of these fibres. LD number increased in the peripheral region of type IIa fibres (+57%; $P = 0.014$) whereas there were no differences in the peripheral region of type IIx fibres. There were no changes in LD number in the central region of type IIa fibres ($P = 0.376$) and type IIx fibres ($P = 0.140$) after the HFHC diet.

PLIN protein expression

PLIN2

At baseline, PLIN2 protein expression (expressed as percentage of fibre stained) was significantly greater in type I fibres in comparison to type IIa ($P = 0.048$) and type IIx fibres ($P = 0.019$), however, there was no difference between type IIa and type IIx fibres ($P = 0.112$; Figure 5A). There were also no differences in PLIN2 protein expression between the central and peripheral region. Furthermore, following the HFHC diet there was no changes in PLIN2 protein expression in any fibre types or any region.

PLIN3

PLIN3 protein expression was higher in type I fibres compared to type IIx fibres only (P = 0.021; Figure 5B), whereas there were no differences between type IIa and IIx fibres. There were also no differences in PLIN3 protein expression between the peripheral and central region of the muscle fibre (Figure 5B). Following the HFHC diet there was an increase in PLIN3 protein expression in type I fibres only (+50%; P = 0.010), occurring in both the peripheral (+35%) and central region of the muscle fibre (+58%). The increase in type I fibres resulted in a significantly higher PLIN3 protein expression in type I fibres compared to type IIa (P = 0.001) and IIx (P < 0.001) after the HFHC diet. Although overall PLIN3 protein expression in type IIa fibres did not change there was an increase in PLIN3 protein expression in the peripheral region of type IIa fibres (+58%; P = 0.043).

PLIN5

At baseline, there was significantly more PLIN5 protein expression in type I fibres compared to type IIa (P = 0.001) and type IIx (P = 0.001), although there were no differences between type IIa and IIx fibres (P = 1.000; Figure 5C). PLIN5 protein expression was also greater in the peripheral region of the muscle fibres compared to the central region (P = 0.001). Overall PLIN5 protein expression did not increase with the HFHC diet (P = 0.342).

LD and PLIN protein colocalisation

Colocalisation analysis was only conducted on type I and IIa fibres due to insufficient type IIx fibres being acquired during image capture.

PLIN2

At baseline, the fraction of PLIN2 colocalising to LD was higher in type I fibres (0.41 ± 0.14) compared to type IIa (0.31 ± 0.13 ; P = 0.001), with no differences between the central region (0.36 ± 0.15) and the peripheral region (0.36 ± 0.15; P = 0.918). Following the HFHC diet

there was an increase in the fraction of PLIN2 colocalising to LD in type I fibres only (+26%; P =0.001), due to increases in both the peripheral (32%; P = 0.006) and central regions (+25%; P = 0.031). At baseline, type I fibres had significantly more PLIN2+ LD in comparison to type IIa fibres (P = 0.001) and there was more PLIN2+ LD in the peripheral region of muscle fibres compared to the central region (P < 0.001; Figure 6A). Following the HFHC diet there was an increase in PLIN2+ LD in type I fibres only (+80%; P = 0.005; Figure 6A), due to increases in both the peripheral (+78%; P = 0.002) and the central regions (+83%; P = 0.017; Figure 6A). There were more PLIN2- LD in type I compared to type IIa fibres (P < 0.001), but no difference in the proportion of PLIN2- LD in the peripheral and central region of muscle fibres at baseline (P = 0.446; Figure 7B), and this relationship did not change with the HFHC diet. At baseline, the peripheral region of muscle fibres had higher amounts of free PLIN2 (0.065 ± 0.027 μm^{-2}) compared to central (0.041 ± 0.021 μm^{-2}; P < 0.001), however there were no differences between fibre types, and this was unaltered after the HFHC diet. In summary, in type I fibres there was an increase in the fraction of PLIN2 colocalising to LD which resulted in an increase in PLIN2+ LD.

PLIN3

At baseline, the fraction of PLIN3 colocalising to LD was higher in type I fibres (0.32 ± 0.12) compared to type IIa (0.22 ± 0.13; P < 0.001), with no differences between the central region (0.26 ± 0.14) and the peripheral region (0.28 ± 0.13; P = 0.628). Following the HFHC diet there was an increase in the fraction of PLIN3 colocalising to LD in both type I fibres (+44%; P < 0.001) and type IIa fibres (+39%; P = 0.002). In type I fibres this was due to increases in both the peripheral (60%; P < 0.001) and central regions (29%; P = 0.012). In type IIa fibres however only the central region observed a significant increase (66%; P = 0.001). Type I fibres had significantly more PLIN3+ and PLIN3- LD in comparison to type IIa fibres (P < 0.001), but the proportion of PLIN3+ and PLIN3- LD in the peripheral and central region of

muscle fibres was not different (P = 0.219; Figure 6C-D). The HFHC diet did not change the number of PLIN3+ LD. However, following the HFHC diet there was a significant increase in PLIN3- LD in both type I (+58%; P < 0.001) and type IIa fibres (+43%; P = 0.017; Figure 6D). In type I fibres the increase was observed in both the peripheral (+69%; P < 0.001) and central regions (+47%; P = 0.001), whereas in type IIa fibres there was only an increase in the peripheral region (+40%; P = 0.026, Figure 7D). There was no difference in free PLIN3 in any fibre type or any region at baseline. The HFHC diet reduced free PLIN3 in type I fibres exclusively (0.071 ± 0.021 to 0.050 ± 0.028 μm^{-2}; P = 0.010) which occurred in the peripheral region only (-36%; P = 0.002). To recap, there was an increase in the fraction of PLIN3 colocalising to LD in both type I and IIa fibres, but this did not result in an increase in PLIN3+ LD.

PLIN5

At baseline, the fraction of PLIN5 colocalising to LD was similar between type I fibres (0.56 ± 0.14) and type IIa (0.49 ± 0.16; P = 0.095), with no differences between the central region (0.54 ± 0.15) and the peripheral region (0.50 ± 0.15; P = 0.416). Following the HFHC diet there was an increase in the fraction of PLIN5 colocalising to LD in both type I fibres (+27%; P = 0.001) and type IIa fibres (+19%; P = 0.027), due to similar increases in central and peripheral region for both fibre types. There was more PLIN5+ LD in type I compared to type IIa fibres (P < 0.001) and in the peripheral region compared to the central region (P < 0.001), but this relationship was unchanged with the HFHC diet (Figure 6E). The number of PLIN5- LD was not different between fibre types and regions and this was not altered following the HFHC diet (Figure 6F). Free PLIN5 was significantly higher in type I (0.048 ± 0.026 μm^{-2}) in comparison to type IIa fibres (0.032 ± 0.019 μm^{-2}; P = 0.003) and in the peripheral region across fibre types (0.049 ± 0.026 μm^{-2}) compared to the central region (0.031 ± 0.018 μm^{-2}; P < 0.001) and this was unaltered with the HFHC diet. In summary,

394 there was an increase in the fraction of PLIN5 colocalising to LD in both type I and IIa fibres,
395 but this did not alter the number of PLIN5+ LD.

COXIV fluorescence intensity

Mitochondria

COXIV protein expression, representing mitochondrial content, displayed a hierarchical fibre type distribution such that type I fibres (64 ± 29AU) was significantly higher in comparison to type IIa (55 ± 25 AU; $P = 0.034$), and type IIa fibres was significantly higher than type IIx fibres (52 ± 24; $P = 0.030$). There was also greater COXIV protein expression in the peripheral region (70 ± 30 AU) compared to the central region across fibres (55 ± 26-AU; $P < 0.001$). The HFHC diet did not change COXIV protein expression in any fibre type or any region.

Discussion

The overlying aim of the present study was to examine the effects of consuming a HFHC diet for 7 days on intramuscular lipid storage and the expression and subcellular distribution of key proteins related to lipid metabolism, in healthy lean individuals. The first major finding was that the HFHC diet increased IMTG content exclusively in type I fibres, due to an increase in both LD size and number whilst whole muscle levels of ceramides and DAGs were unaltered. PLIN3 was the only PLIN protein to exhibit increased expression after 7 days HFHC diet, but this was not mirrored by an increase in PLIN3+ LD. Rather, we observed an increased number of PLIN2+ LD in type I fibres. We review these adaptations in the context of our previous findings showing a decrease in glucose clearance and reduced glycaemic control, despite maintenance of normal skeletal muscle insulin signalling in these subjects (Parry *et al.*, 2019). Together, the data shows that a 7-day HFHC diet leads to increased IMTG storage alongside, increases in PLIN3 protein expression and PLIN2+ LD. Moreover, the increase in IMTG may contribute to the maintenance of skeletal muscle insulin signalling by minimising the accumulation of inhibitory lipid metabolites.

As previously mentioned our healthy lean subjects in this study experienced a decrease in glucose clearance and reduced glycaemic control after 7 days on the HFHC diet, without impairments in the phosphorylation of key insulin signalling intermediates (Akt and AS160) (Parry *et al.*, 2019). Accumulation of ceramide in skeletal muscle dephosphorylates Akt via activation of protein phosphatase 2A (Stratford *et al.*, 2004). There is some contention as to DAG's role in the mechanisms leading to skeletal muscle insulin resistance (Amati *et al.*, 2011; Chow *et al.*, 2014). Despite this, certain DAG species have been shown to activate novel PKC isoforms which phosphorylate IRS-1 on serine residues and subsequently inhibit IRS-1 tyrosine

phosphorylation (Yu *et al.*, 2002; Szendroedi *et al.*, 2014), and therefore downstream activation of Akt and AS160. Thus, the finding that the HFHC diet did not affect either ceramide or DAG concentrations is entirely in keeping with the observation of normal phosphorylation of Akt and AS160.

The absence of any alterations in fasting ceramide and DAG concentrations is indicative of dietary FA instead being directed stored as IMTG, if not directed to mitochondria for β-oxidation. First, we observed no differences in whole muscle TAG levels in response to the HFHC diet, which is in contrast to a recent study showing that 5 days of a HFHC diet augmented whole muscle TAG (Gemmink *et al.*, 2017). However, it is now well established that IMTG content can change in a fibre type-specific manner (Shepherd *et al.*, 2012, 2013). For example, IMTG accumulation following 6 h lipid infusion during a hyperinsulinaemic-euglycaemic clamp is specific to type I fibres only (Shepherd *et al.*, 2017). Therefore, we investigated fibre-type specific changes in IMTG content and demonstrate for the first time that a short-term HFHC diet augments IMTG content exclusively in type I fibres. This finding is perhaps unsurprising considering that type I fibres are characterised by a higher mitochondrial content, a greater abundance of lipolytic regulatory proteins, and an enhanced ability to utilise IMTG stores during moderate-intensity exercise (Shepherd *et al.*, 2013; Watt & Cheng, 2017). Therefore, type I fibres are appreciably more equipped to store an influx of dietary FA as IMTG. When muscle lipid content was determined from whole muscle homogenates, there was no difference in overall TAG levels from pre to post HFHC diet. It is possible however that these measurements may have been confounded by the presence of extramyocellular LDs (Guo, 2001). Whilst the bulk of TAG in mammalian cells is stored in LD (Wolins *et al.*, 2001; Kuramoto *et al.*, 2012), particularly in the fasted state (Kuramoto *et al.*, 2012), this has yet to be confirmed in skeletal

muscle. Therefore, although we observed an increase in the amount of TAG stored in LD in type I fibres, we cannot exclude the possibility that extra-LD TAG levels were unchanged but could not be measured on a fibre-type specific basis with the current methodology. Type I fibres also only account for approximately 40% of all fibres in the *v. lateralis* muscle of young participants (Staron et al., 2000). It is possible, therefore, that the observed increase in IMTG in type I fibres only may not lead to an overall increase in whole-muscle TAG concentrations.

We also examined changes in IMTG content on a subcellular-specific basis, as well as exploring adaptations to LD morphology. In this respect, increased IMTG content in type I fibres following the HFHC diet occurred in both the peripheral and central region of the fibres and was due to an increase in both LD size and number. Seven days on the HFHC diet also augmented IMTG content, specifically in the peripheral region of both type II fibres which was again due to elevations in both LD size and number. Interestingly, HFHC diet increased LD size in the central region of both type II fibres, although this did not result in increased IMTG content. These distinct patterns of fibre and region-specific IMTG accumulation and changes in LD morphology are the first of their kind in the literature. Moreover, they are indicative of the progression of IMTG accumulation in muscle, whereby lipid accumulates in type I fibres prior to type II-fibres, changes in LD size precede an increase in LD number, and this occurs in the peripheral region of the cell before the central region.

Increased IMTG content near the plasma membrane of muscle fibres has been associated with insulin resistance (Chee *et al.*, 2016) particularly if IMTG is stored in larger LD (Nielsen *et al.*, 2017; Daemen *et al.*, 2018). Accumulation of IMTG close to the plasma membrane may be detrimental due to the close proximity to key components of the insulin signalling cascade. In particular, increases in LD size rather than number near the plasma membrane will be less

favourable because larger LD have a lower surface area to volume ratio which is proposed to result in lower IMTG turnover and subsequent accumulation of lipid metabolites. In this study, the peripheral region was defined as an area within the muscle fibres that was distinct from the central region of the cell but in close proximity to the plasma membrane and therefore near to insulin signalling and trafficking of FA into the myocyte. The predominant increase in IMTG stores occurred in type I fibres and this was accountable to an increase in LD size and number in both the peripheral and central regions.

During LD expansion the increased distance between phospholipid molecules recruits specific proteins via increased surface tensions (Krahmer *et al.*, 2011). This recruitment has been proposed to be a mechanism of metabolic regulation (Hesselink *et al.*, 2017). Consistent with this hypothesis, Gemmink *et al.* (2016) found that LD size and number increased following acute elevation of FFA from prolonged fasting. Importantly though, those LDs that increased in size and number were also labelled with PLIN5. Furthermore, the individuals who had the largest increase in IMTG content also exhibited the smallest reduction in insulin sensitivity (Gemmink *et al.*, 2016). Therefore, larger LDs may not necessarily impede insulin sensitivity if they are decorated with PLIN proteins.

In the present study, PLIN3 protein expression increased specifically in type I fibres following the HFHC diet. PLIN3 has been linked to formation of new LD following lipid loading in cultured differentiated adipocytes (Wolins *et al.*, 2005). If a similar role exists in skeletal muscle, we might have expected to see an increase in PLIN3+ LD following the HFHC diet; however, only an increase in PLIN3- LD was observed. There was, however, a reduction in free PLIN3 in type I fibres with an increase in the fraction of PLIN3 colocalising to LD. Taken together, these data indicate that PLIN3 is targeted to LD that already have PLIN3 associated and therefore

suggests that PLIN3 supports LD growth and stability, rather than increase in LD number in skeletal muscle. Whether having more PLIN3 localised to the LD supports greater IMTG mobilisation is not yet known. However, PLIN3 has also been observed in the mitochondria in skeletal muscle (Ramos *et al.*, 2014) and PLIN3 knockdown in primary myotubes strongly reduces FA oxidation (Covington *et al.*, 2015). We therefore cannot exclude the possibility that the increase in PLIN3 was related to mitochondrial adaptations.

Despite there not being an increase in PLIN2 protein content, there was an increase in PLIN2+ LD in type I fibres. This occurred without a change in free PLIN2, but with an increase in the fraction of PLIN2 colocalising to LD in type I fibres. Together, this data suggests that the pre-existing pool of PLIN2 that is already localised to LD is redistributed to newly formed LD following the HFHC diet. Previous research reported an increase in PLIN2+ LD without increases in PLIN2 protein expression in trained individuals that underwent lipid infusion (Shepherd *et al.*, 2017), indicating that when there is sufficient PLIN2 in muscle fibres it can be redistributed to an expanding LD pool. PLIN2 is associated with LD biogenesis primarily in adipocytes (Wolins *et al.*, 2005) and murine fibroblasts (Imamura *et al.*, 2002), and PLIN2 is localised at clusters in the cytoplasmic leaflet of the endoplasmic reticulum where LD biogenesis occurs (Robenek *et al.*, 2006). Muscle-specific overexpression of PLIN2 increases IMTG storage in rats fed a high-fat diet without accumulation of lipid metabolite DAG (Bosma *et al.*, 2012). Therefore, newly-formed LD may be labelled with PLIN2 leading to an increase in PLIN2+ LD, and theoretically this may support the storage of FA as IMTG rather than DAG.

There was an increase in the fraction of PLIN5 colocalising to LD in type I fibres which occurred without any change in PLIN5+ LD This is indicative of PLIN5 colocalising to LD that already have PLIN5 associated (PLIN5+LD), rather than transforming PLIN5- LD into PLIN5+

LD. PLIN5 has been primarily associated with oxidative capacity (Koves *et al.*, 2013) and IMTG oxidation. For example PLIN5 protein expression is upregulated following endurance training (Louche *et al.*, 2013; Shepherd *et al.*, 2013) and during a moderate-intensity bout of exercise PLIN5+ LD are preferentially used (Shepherd *et al.*, 2013). Recent findings suggest that PLIN5 protein expression and lipid area fraction covered by PLIN5+ LD correlated positively with VO_{2max} and *ex vivo* fatty acid oxidation but not insulin sensitivity (Gemmink *et al.*, 2018). Increased LD content due to increases in PLIN5+ LD are associated with blunted reductions in insulin sensitivity following acute FFA elevation from prolonged fasting (Gemmink *et al.*, 2016). Given PLIN5's proposed role in regulating IMTG lipolysis, in the current study the increased fraction of PLIN5 to LD may function to support the consistent turnover of PLIN5+ LD pool and thus help to minimise accumulation of lipid metabolites.

The use of previously validated immunofluorescence microscopy techniques (Shepherd *et al.*, 2012, 2013; Shepherd *et al.*, 2017) to examine fibre-type and region specific changes in IMTG content and PLIN protein expression, in addition to colocalisation between PLIN proteins to LD following the HFHC diet is a clear strength of this study. We should acknowledge though that the colocalisation analysis was only able to investigate the association between a single PLIN protein with LD. We cannot exclude the possibility, therefore, that LD have multiple PLIN proteins colocalised to them. For example, it is possible that the increases observed in PLIN3-LD and PLIN5- LD could be due to increases in LD coated with PLIN2. PLIN- LDs may also be newly formed LD that did not have enough PLIN associated to them to be detected by the lower detection limit of the microscope. Whether PLIN proteins work together or in isolation in regulating LD dynamics remains an avenue for future research. Studies employing subcellular fractionation in heart muscle, liver and adipose tissue have demonstrated that a large proportion

543 of PLIN proteins exist in the soluble cytosolic fraction (Harris *et al.*, 2012; Kuramoto *et al.*,
544 2012). Cross-sectional images of muscle fibres in the current study showed that some of the
545 cytosolic PLIN proteins appear in clusters throughout the cytosol and a proportion appeared as a
546 diffuse stain throughout the muscle fibre. Because our analysis applies thresholds based on a
547 fluorescence intensity to quantify PLIN proteins on cross-sectional images, we may have
548 underestimated the total amount of soluble cytosolic PLINs. Due to limitations in subcellular
549 fractionation in skeletal muscle tissue there is no existing information on the proportion of the
550 soluble cytosolic PLIN pool in skeletal muscle and we therefore cannot determine the
551 discrepancy between the imaging quantification method and the total amount existing in the
552 cytosolic muscle fibre.

553 Contrary to previous research (Garcia-Roves *et al.*, 2007; Hancock *et al.*, 2008), mitochondrial
554 content was not increased following the HFHC diet. Increased mitochondrial content is an
555 adaptation to enhance fatty acid β-oxidation fat oxidation especially in the face of increased FA
556 supply (Jain *et al.*, 2014). The lack of change in mitochondrial content in the current study could
557 indicate that there was sufficient mitochondria already in muscle fibres in our physically active
558 cohort to accommodate any required increase in FA oxidation. Transmission electron
559 microscopy and confocal immunofluorescence microscopy have confirmed that LDs are in close
560 proximity to mitochondria in skeletal muscle (Hoppeler *et al.*, 1999; Shaw *et al.*, 2008).
561 Younger, more insulin- sensitive individuals also have a greater fraction of LD in contact with
562 the mitochondria (Crane *et al.*, 2010). A limitation of the current study is that we could not
563 measure the spatial interaction between mitochondria and LD because of sample size limitations.
564 It is important to note that this spatial interaction, may have contributed to the observed increase
565 in FA oxidation in the absence of an increase in mitochondrial content.

The present research was conducted in lean healthy individual for an acute period of 7-days. Future research should aim to investigate the effects of a HFHC diet on lipid storage and skeletal muscle insulin resistance in older, sedentary and overweight/obese population who are more susceptible to develop type 2 diabetes. Furthermore, extending the dietary period to a more long-term setting would advance our understanding of the chronic effect of a HFHC diet and the mechanisms leading to skeletal muscle insulin resistance under these conditions.

In conclusion, the present study has generated novel evidence that 7 days on a HFHC diet induces fibre type-specific increases in IMTG content and PLIN3 protein expression. Whist there was an increase in PLIN3 colocalising to LD, there was no change in PLIN3+ LD indicative of PLIN3 being directed to previously formed PLIN3+ LD rather than forming new PLIN3+ LD. In contrast the HFHC diet increased the number of PLIN2+ LD showing a redistribution of PLIN2 to LD. We propose that the increase in IMTG reduces accumulation of lipid metabolites (DAG and ceramides), thus helping to maintain the insulin signalling pathway in skeletal muscle fibres as observed in our recent study (Parry *et al.*, 2019).

References

Amati F, Dube JJ, Alvarez-Carnero E, Edreira MM, Chomentowski P, Coen PM, Switzer GE, Bickel PE, Stefanovic-Racic M, Toledo FG & Goodpaster BH. (2011). Skeletal muscle triglycerides, diacylglycerols, and ceramides in insulin resistance: another paradox in endurance-trained athletes? *Diabetes* **60,** 2588-2597.

Amrutkar M, Cansby E, Nunez-Duran E, Pirazzi C, Stahlman M, Stenfeldt E, Smith U, Boren J & Mahlapuu M. (2015). Protein kinase STK25 regulates hepatic lipid partitioning and progression of liver steatosis and NASH. *Faseb J* **29,** 1564-1576.

Bakker LE, van Schinkel LD, Guigas B, Streefland TC, Jonker JT, van Klinken JB, van der Zon GC, Lamb HJ, Smit JW, Pijl H, Meinders AE & Jazet IM. (2014). A 5-day high-fat, high-calorie diet impairs insulin sensitivity in healthy, young South Asian men but not in Caucasian men. *Diabetes* **63,** 248-258.

595 Bergström J. (1975). Percutaneous needle biopsy of skeletal muscle in physiological and clinical
596 research. *Scand J Clin Lab Invest* **35,** 609-616.

597
598 Bersuker K & Olzmann JA. (2017). Establishing the lipid droplet proteome: Mechanisms of lipid
599 droplet protein targeting and degradation. *Biochim Biophys Acta Mol Cell Biol Lipids*
600 **1862,** 1166-1177.

601
602 Boden G, Chen X, Ruiz J, White JV & Rossetti L. (1994). Mechanisms of fatty acid-induced
603 inhibition of glucose uptake. *J Clin Invest* **93,** 2438-2446.

604
605 Bosma M, Hesselink MK, Sparks LM, Timmers S, Ferraz MJ, Mattijssen F, van Beurden D,
606 Schaart G, de Baets MH, Verheyen FK, Kersten S & Schrauwen P. (2012). Perilipin 2
607 improves insulin sensitivity in skeletal muscle despite elevated intramuscular lipid levels.
608 *Diabetes* **61,** 2679-2690.

609
610 Bosma M, Sparks LM, Hooiveld GJ, Jorgensen JA, Houten SM, Schrauwen P, Kersten S &
611 Hesselink MK. (2013). Overexpression of PLIN5 in skeletal muscle promotes oxidative
612 gene expression and intramyocellular lipid content without compromising insulin
613 sensitivity. *Biochim Biophys Acta* **1831,** 844-852.

614
615 Chee C, Shannon CE, Burns A, Selby AL, Wilkinson D, Smith K, Greenhaff PL & Stephens FB.
616 (2016). Relative Contribution of Intramyocellular Lipid to Whole-Body Fat Oxidation Is
617 Reduced With Age but Subsarcolemmal Lipid Accumulation and Insulin Resistance Are
618 Only Associated With Overweight Individuals. *Diabetes* **65,** 840-850.

619
620 Chow LS, Mashek DG, Austin E, Eberly LE, Persson XM, Mashek MT, Seaquist ER & Jensen
621 MD. (2014). Training status diverges muscle diacylglycerol accumulation during free
622 fatty acid elevation. *Am J Physiol Endocrinol Metab* **307,** E124-131.

623
624 Covington JD, Noland RC, Hebert RC, Masinter BS, Smith SR, Rustan AC, Ravussin E &
625 Bajpeyi S. (2015). Perilipin 3 Differentially Regulates Skeletal Muscle Lipid Oxidation in
626 Active, Sedentary, and Type 2 Diabetic Males. *J Clin Endocrinol Metab* **100,** 3683-3692.

627
628 Crane JD, Devries MC, Safdar A, Hamadeh MJ & Tarnopolsky MA. (2010). The effect of aging
629 on human skeletal muscle mitochondrial and intramyocellular lipid ultrastructure. *J*
630 *Gerontol A Biol Sci Med Sci* **65,** 119-128.

631
632 Daemen S, Gemmink A, Brouwers B, Meex RCR, Huntjens PR, Schaart G, Moonen-Kornips E,
633 Jorgensen J, Hoeks J, Schrauwen P & Hesselink MKC. (2018). Distinct lipid droplet
634 characteristics and distribution unmask the apparent contradiction of the athlete's
635 paradox. *Mol Metab* **17,** 71-81.

636
637 DeFronzo RA & Tripathy D. (2009). Skeletal muscle insulin resistance is the primary defect in
638 type 2 diabetes. *Diabetes Care* **32 Suppl 2,** S157-163.

Ferrannini E, Smith JD, Cobelli C, Toffolo G, Pilo A & DeFronzo RA. (1985). Effect of insulin on the distribution and disposition of glucose in man. *J Clin Invest* **76,** 357-364.

Garcia-Roves P, Huss JM, Han DH, Hancock CR, Iglesias-Gutierrez E, Chen M & Holloszy JO. (2007). Raising plasma fatty acid concentration induces increased biogenesis of mitochondria in skeletal muscle. *Proc Natl Acad Sci U S A* **104,** 10709-10713.

Gemmink A, Bakker LE, Guigas B, Kornips E, Schaart G, Meinders AE, Jazet IM & Hesselink MK. (2017). Lipid droplet dynamics and insulin sensitivity upon a 5-day high-fat diet in Caucasians and South Asians. *Sci Rep* **7,** 42393.

Gemmink A, Bosma M, Kuijpers HJ, Hoeks J, Schaart G, van Zandvoort MA, Schrauwen P & Hesselink MK. (2016). Decoration of intramyocellular lipid droplets with PLIN5 modulates fasting-induced insulin resistance and lipotoxicity in humans. *Diabetologia* **59,** 1040-1048.

Gemmink A, Daemen S, Brouwers B, Huntjens PR, Schaart G, Moonen-Kornips E, Jorgensen J, Hoeks J, Schrauwen P & Hesselink MKC. (2018). Dissociation of intramyocellular lipid storage and insulin resistance in trained athletes and type 2 diabetes patients; involvement of perilipin 5? *J Physiol* **596,** 857-868.

Goodpaster BH, He J, Watkins S & Kelley DE. (2001). Skeletal muscle lipid content and insulin resistance: evidence for a paradox in endurance-trained athletes. *J Clin Endocrinol Metab* **86,** 5755-5761.

Guo Z. (2001). Triglyceride content in skeletal muscle: variability and the source. *Anal Biochem* **296,** 1-8.

Hancock CR, Han DH, Chen M, Terada S, Yasuda T, Wright DC & Holloszy JO. (2008). High-fat diets cause insulin resistance despite an increase in muscle mitochondria. *Proc Natl Acad Sci U S A* **105,** 7815-7820.

Harris LA, Shew TM, Skinner JR & Wolins NE. (2012). A single centrifugation method for isolating fat droplets from cells and tissues. *J Lipid Res* **53,** 1021-1025.

Hesselink MKC, Daemen S, van Polanen N & Gemmink A. (2017). What are the benefits of being big? *J Physiol* **595,** 5409-5410.

Hoppeler H, Billeter R, Horvath PJ, Leddy JJ & Pendergast DR. (1999). Muscle structure with low- and high-fat diets in well-trained male runners. *Int J Sports Med* **20,** 522-526.

Hulston CJ, Churnside AA & Venables MC. (2015). Probiotic supplementation prevents high-fat, overfeeding-induced insulin resistance in human subjects. *Br J Nutr* **113,** 596-602.

683
684 Imamura M, Inoguchi T, Ikuyama S, Taniguchi S, Kobayashi K, Nakashima N & Nawata H.
685 (2002). ADRP stimulates lipid accumulation and lipid droplet formation in murine
686 fibroblasts. *Am J Physiol Endocrinol Metab* **283,** E775-783.

687
688 Itani SI, Ruderman NB, Schmieder F & Boden G. (2002). Lipid-induced insulin resistance in
689 human muscle is associated with changes in diacylglycerol, protein kinase C, and
690 IkappaB-alpha. *Diabetes* **51,** 2005-2011.

691
692 Jain SS, Paglialunga S, Vigna C, Ludzki A, Herbst EA, Lally JS, Schrauwen P, Hoeks J, Tupling
693 AR, Bonen A & Holloway GP. (2014). High-fat diet-induced mitochondrial biogenesis is
694 regulated by mitochondrial-derived reactive oxygen species activation of CaMKII.
695 *Diabetes* **63,** 1907-1913.

696
697 Katz LD, Glickman MG, Rapoport S, Ferrannini E & DeFronzo RA. (1983). Splanchnic and
698 peripheral disposal of oral glucose in man. *Diabetes* **32,** 675-679.

699
700 Kelley DE, Goodpaster B, Wing RR & Simoneau JA. (1999). Skeletal muscle fatty acid
701 metabolism in association with insulin resistance, obesity, and weight loss. *Am J Physiol*
702 **277,** E1130-1141.

703
704 Kleinert M, Parker BL, Chaudhuri R, Fazakerley DJ, Serup A, Thomas KC, Krycer JR, Sylow L,
705 Fritzen AM, Hoffman NJ, Jeppesen J, Schjerling P, Ruegg MA, Kiens B, James DE &
706 Richter EA. (2016). mTORC2 and AMPK differentially regulate muscle triglyceride
707 content via Perilipin 3. *Mol Metab* **5,** 646-655.

708
709 Koves TR, Sparks LM, Kovalik JP, Mosedale M, Arumugam R, DeBalsi KL, Everingham K,
710 Thorne L, Phielix E, Meex RC, Kien CL, Hesselink MK, Schrauwen P & Muoio DM.
711 (2013). PPARgamma coactivator-1alpha contributes to exercise-induced regulation of
712 intramuscular lipid droplet programming in mice and humans. *J Lipid Res* **54,** 522-534.

713
714 Krahmer N, Guo Y, Wilfling F, Hilger M, Lingrell S, Heger K, Newman HW, Schmidt-Supprian M,
715 Vance DE, Mann M, Farese RV, Jr. & Walther TC. (2011). Phosphatidylcholine
716 synthesis for lipid droplet expansion is mediated by localized activation of
717 CTP:phosphocholine cytidylyltransferase. *Cell Metab* **14,** 504-515.

718
719 Kuramoto K, Okamura T, Yamaguchi T, Nakamura TY, Wakabayashi S, Morinaga H, Nomura
720 M, Yanase T, Otsu K, Usuda N, Matsumura S, Inoue K, Fushiki T, Kojima Y, Hashimoto
721 T, Sakai F, Hirose F & Osumi T. (2012). Perilipin 5, a lipid droplet-binding protein,
722 protects heart from oxidative burden by sequestering fatty acid from excessive oxidation.
723 *J Biol Chem* **287,** 23852-23863.

724
725 Laurens C, Bourlier V, Mairal A, Louche K, Badin PM, Mouisel E, Montagner A, Marette A,
726 Tremblay A, Weisnagel JS, Guillou H, Langin D, Joanisse DR & Moro C. (2016).

Perilipin 5 fine-tunes lipid oxidation to metabolic demand and protects against lipotoxicity in skeletal muscle. *Sci Rep* **6,** 38310.

Lofgren L, Forsberg GB & Stahlman M. (2016). The BUME method: a new rapid and simple chloroform-free method for total lipid extraction of animal tissue. *Sci Rep* **6,** 27688.

Louche K, Badin PM, Montastier E, Laurens C, Bourlier V, de Glisezinski I, Thalamas C, Viguerie N, Langin D & Moro C. (2013). Endurance exercise training up-regulates lipolytic proteins and reduces triglyceride content in skeletal muscle of obese subjects. *J Clin Endocrinol Metab* **98,** 4863-4871.

Lundsgaard AM, Sjoberg KA, Hoeg LD, Jeppesen J, Jordy AB, Serup AK, Fritzen AM, Pilegaard H, Myrmel LS, Madsen L, Wojtaszewski JFP, Richter EA & Kiens B. (2017). Opposite Regulation of Insulin Sensitivity by Dietary Lipid Versus Carbohydrate Excess. *Diabetes* **66,** 2583-2595.

Mifflin MD, St Jeor ST, Hill LA, Scott BJ, Daugherty SA & Koh YO. (1990). A new predictive equation for resting energy expenditure in healthy individuals. *The American journal of clinical nutrition* **51,** 241-247.

Murphy RC, James PF, McAnoy AM, Krank J, Duchoslav E & Barkley RM. (2007). Detection of the abundance of diacylglycerol and triacylglycerol molecular species in cells using neutral loss mass spectrometry. *Anal Biochem* **366,** 59-70.

Nielsen J, Christensen AE, Nellemann B & Christensen B. (2017). Lipid droplet size and location in human skeletal muscle fibers are associated with insulin sensitivity. *Am J Physiol Endocrinol Metab* **313,** E721-E730.

Parry SA, Smith JR, Corbett TRB, Woods RM & Hulston CJ. (2017). Short-term, high-fat overfeeding impairs glycaemic control but does not alter gut hormone responses to a mixed meal tolerance test in healthy, normal-weight individuals. *Brit J Nutr* **117,** 48-55.

Parry SA, Turner MC, Woods RM, James LJ, Ferguson RA, Cocks M, Whytock KL, Strauss JA, Shepherd SO, Wagenmakers AJM, van Hall G & Hulston CJ. (2019). High-fat overfeeding impairs peripheral glucose metabolism and muscle microvascular eNOS Ser1177 phosphorylation. *J Clin Endocrinol Metab*.

Ramos SV, MacPherson RE, Turnbull PC, Bott KN, LeBlanc P, Ward WE & Peters SJ. (2014). Higher PLIN5 but not PLIN3 content in isolated skeletal muscle mitochondria following acute in vivo contraction in rat hindlimb. *Physiol Rep* **2**.

Robenek H, Hofnagel O, Buers I, Robenek MJ, Troyer D & Severs NJ. (2006). Adipophilin-enriched domains in the ER membrane are sites of lipid droplet biogenesis. *J Cell Sci* **119,** 4215-4224.

Shaw CS, Jones DA & Wagenmakers AJ. (2008). Network distribution of mitochondria and lipid droplets in human muscle fibres. *Histochem Cell Biol* **129,** 65-72.

Shaw CS, Shepherd SO, Wagenmakers AJM, Hansen D, Dendale P & van Loon LJC. (2012). Prolonged exercise training increases intramuscular lipid content and perilipin 2 expression in type I muscle fibers of patients with type 2 diabetes. *Am J Physiol-Endoc M* **303,** E1158-E1165.

Shepherd SO, Cocks M, Tipton KD, Ranasinghe AM, Barker TA, Burniston JG, Wagenmakers AJ & Shaw CS. (2012). Preferential utilization of perilipin 2-associated intramuscular triglycerides during 1 h of moderate-intensity endurance-type exercise. *Exp Physiol* **97,** 970-980.

Shepherd SO, Cocks M, Tipton KD, Ranasinghe AM, Barker TA, Burniston JG, Wagenmakers AJ & Shaw CS. (2013). Sprint interval and traditional endurance training increase net intramuscular triglyceride breakdown and expression of perilipin 2 and 5. *J Physiol* **591,** 657-675.

Shepherd SO, Cocks M, Tipton KD, Witard OC, Ranasinghe AM, Barker TA, Wagenmakers AJ & Shaw CS. (2014). Resistance training increases skeletal muscle oxidative capacity and net intramuscular triglyceride breakdown in type I and II fibres of sedentary males. *Exp Physiol* **99,** 894-908.

Shepherd SO, Strauss JA, Wang Q, Dube JJ, Goodpaster B, Mashek DG & Chow LS. (2017). Training alters the distribution of perilipin proteins in muscle following acute free fatty acid exposure. *J Physiol* **595,** 5587-5601.

Staron RS, Hagerman FC, Hikida RS, Murray TF, Hostler DP, Crill MT, Ragg KE & Toma K. (2000). Fiber type composition of the vastus lateralis muscle of young men and women. *J Histochem Cytochem* **48,** 623-629.

Stratford S, Hoehn KL, Liu F & Summers SA. (2004). Regulation of insulin action by ceramide: dual mechanisms linking ceramide accumulation to the inhibition of Akt/protein kinase B. *J Biol Chem* **279,** 36608-36615.

Strauss JA, Shaw CS, Bradley H, Wilson OJ, Dorval T, Pilling J & Wagenmakers AJ. (2016). Immunofluorescence microscopy of SNAP23 in human skeletal muscle reveals colocalization with plasma membrane, lipid droplets, and mitochondria. *Physiol Rep* **4**.

Szendroedi J, Yoshimura T, Phielix E, Koliaki C, Marcucci M, Zhang D, Jelenik T, Muller J, Herder C, Nowotny P, Shulman GI & Roden M. (2014). Role of diacylglycerol activation of PKCtheta in lipid-induced muscle insulin resistance in humans. *Proc Natl Acad Sci U S A* **111,** 9597-9602.

van Loon LJ, Koopman R, Manders R, van der Weegen W, van Kranenburg GP & Keizer HA. (2004). Intramyocellular lipid content in type 2 diabetes patients compared with overweight sedentary men and highly trained endurance athletes. *Am J Physiol Endocrinol Metab* **287,** E558-565.

Watt MJ & Cheng Y. (2017). Triglyceride metabolism in exercising muscle. *Biochim Biophys Acta* **1862,** 1250-1259.

Whytock KL, Shepherd SO, Wagenmakers AJM & Strauss JA. (2018). Hormone-sensitive lipase preferentially redistributes to lipid droplets associated with perilipin-5 in human skeletal muscle during moderate-intensity exercise. *J Physiol* **596,** 2077-2090.

Wolins NE, Quaynor BK, Skinner JR, Schoenfish MJ, Tzekov A & Bickel PE. (2005). S3-12, Adipophilin, and TIP47 package lipid in adipocytes. *J Biol Chem* **280,** 19146-19155.

Wolins NE, Rubin B & Brasaemle DL. (2001). TIP47 associates with lipid droplets. *J Biol Chem* **276,** 5101-5108.

Yu C, Chen Y, Cline GW, Zhang D, Zong H, Wang Y, Bergeron R, Kim JK, Cushman SW, Cooney GJ, Atcheson B, White MF, Kraegen EW & Shulman GI. (2002). Mechanism by which fatty acids inhibit insulin activation of insulin receptor substrate-1 (IRS-1)-associated phosphatidylinositol 3-kinase activity in muscle. *J Biol Chem* **277,** 50230-50236.

Funding

Work that was undertaken at Loughborough University was funded by the National Institute for Health Research (NIHR) Leicester Biomedical Research Centre. The views expressed are those of the authors and not necessarily those of the NHS, the NIHR or the Department of Health and Social Care.

Competing interests

The authors declare they have no competing interests.

Author contributions

KLW, SAP, JAS, AJMW, CJH, SOS were responsible for the conception and design of the experiments. SAP, LJJ, RAF and CJH conducted the clinical trial. KLW, SAP, MCT, RMW, MS, JB, JAS, MC and SOS contributed to the analysis and interpretation of the data. KLW, JAS, AJMW and SOS wrote the manuscript. All authors contributed to the manuscript and approved the final version of the manuscript. All persons designated as authors qualify for authorship, and all those who qualify for authorship are listed.

Acknowledgements

There are no acknowledgements

Figures Legends

Figure 1. Image analysis method for assessing IMTG and protein expression in cross-sectional muscle fibres. Images for content analysis were obtained at 1.1x zoom on a 63x 1.4NA confocal microscope. Grey scale images of the cell border identified with laminin (*A*) and of LD stained with BODIPY 493/503 (*D*). Erosion mask of 5 μm applied from the cell border to produce a peripheral region mask (*B*). Peripheral erosion mask inverted to create a mask for the central region of the cell (*C*). Masks B and C were applied to greyscale image of LD to produce extracted images of LD in the peripheral region of the cell (*E*) and the central region of the cell (*F*). Freehand ROI (green line) was manually drawn around central region of the cell to exclude LD from neighbouring cells (*F*). A selected intensity threshold was then applied to extracted images to represent positive signal for LD or PLIN proteins and the data was extracted to reveal percentage of area stained (IMTG and PLINs) as well as LD density (number of LDs expressed relative to area) and LD size (mean area of individual LDs). White bar = 25μm.

Figure 2. Colocalisation analysis between LD and PLIN5. Images for colocalisation analysis were obtained using a 63x 1.4NA confocal microscope at 4x digital zoom at the central and peripheral region of the cell indicated by the two white boxes (*A*). LD were stained with BODIPY 493/503 (green*; B*), PLIN5 was stained red (*C*) and subsequent merged images (*D*) were used to calculate colocalisation. The overlapping area of LD and PLIN5 was extracted (*E*) to calculate the number of PLIN5+ LD and PLIN5- LD relative to the area of interest. White box in images *B*-*E* represent the peripheral area that was analysed when images at the periphery were obtained. White bar = 25μm (*A*) and 5 μm (*B*-*E*). The same method was repeated for colocalisation analysis between LD with PLIN2 and PLIN3.

Figure 3. TAG, DAG and ceramide concentrations in extracts of muscle samples obtained pre and post 7 days HFHC diet. There were no significant changes in overall TAG (A), DAG (B) or ceramide levels (C). 7 Days HFHC diet did not induce changes in any individual DAG species (D) or ceramide species (E).

Figure 4. 7-days HFHC diet induces increases in IMTG content in type I fibres due to increases in LD density and size. 7 days HFHC diet increases type I fibre IMTG content (*A*), LD density (*B*) and LD size (*C*). Representative images of IMTG content pre and post HFHC diet in different fibre types obtained from confocal microscope with a 63x oil immersion objective and 1.1 digital zoom (*D*). Corresponding images of myosin heavy chain (MHC I) (stained red for type I fibres) and myosin heavy chain (MHC IIa) (stained blue for type IIa fibres), any fibres without a positive red or blue stain were assumed to be type IIx fibres (*E*). White bars represent 25 μm.* Significant difference for type I fibres *vs* type IIa and IIx fibres ($P < 0.001$). ‡ Significant difference for HFHC diet ($P < 0.01$). † Significant difference for central *vs* peripheral region ($P < 0.01$). # Significant interaction between fibre type and HFHC diet ($P < 0.001$).

Figure 5. PLIN protein expression after pre and post 7 days HFHC diet. 7 days HFHC diet does not alter PLIN2 (*A*) or PLIN5 (*C*) protein expression but increases PLIN3 protein expression in type I fibres only (*B*). Representative images of PLIN2, PLIN3 and PLIN5 protein expression pre and post HFHC diet in type I fibres obtained from confocal microscope with a 63x oil immersion objective and 1.1 digital zoom (*D*). White bars represent 25 μm *Significant difference for type I fibres *vs* type IIa and IIx fibres ($P < 0.05$). # Significant difference for type I fibres *vs* IIx fibres ($P < 0.05$). † Significant difference for peripheral region vs central region ($P < 0.01$). ‡ Significant difference for HFHC diet ($P < 0.01$).

Figure 6. HFHC diet increases PLIN2+ LD in type I fibres only. 7 days HFHC diet increased PLIN2+ LD in type I fibres (*A*), whilst there were no changes in PLIN3+ LD (*C*) or PLIN5+ LD (*E*). PLIN2- LD (*B*) and PLIN5- LD (*F*) were not altered with the HFHC diet, whereas PLIN3- LD significant increased (*D*).* Significant difference for type I fibres *vs* type IIa ($P < 0.01$). † Significant difference for peripheral region vs central region ($P < 0.01$). Significant difference for peripheral region vs central region ($P < 0.001$). ‡ Significant difference for the HFHC diet ($P < 0.05$). # Significant interaction effect between fibre type and the HFHC diet ($P < 0.001$).

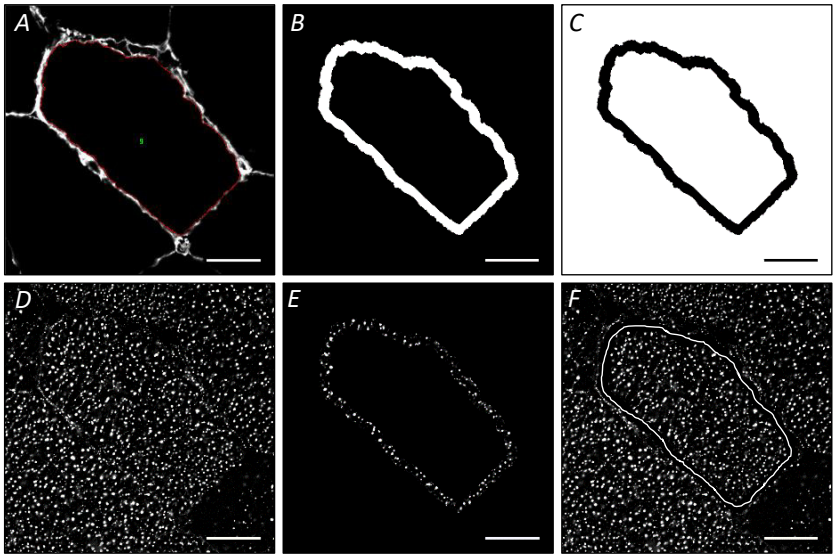
A
B
C
D
E
F

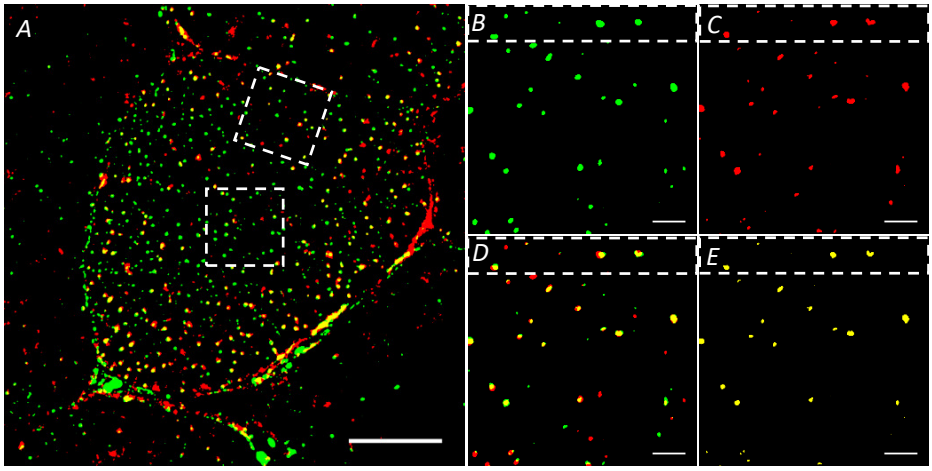
A
B
C
D
E

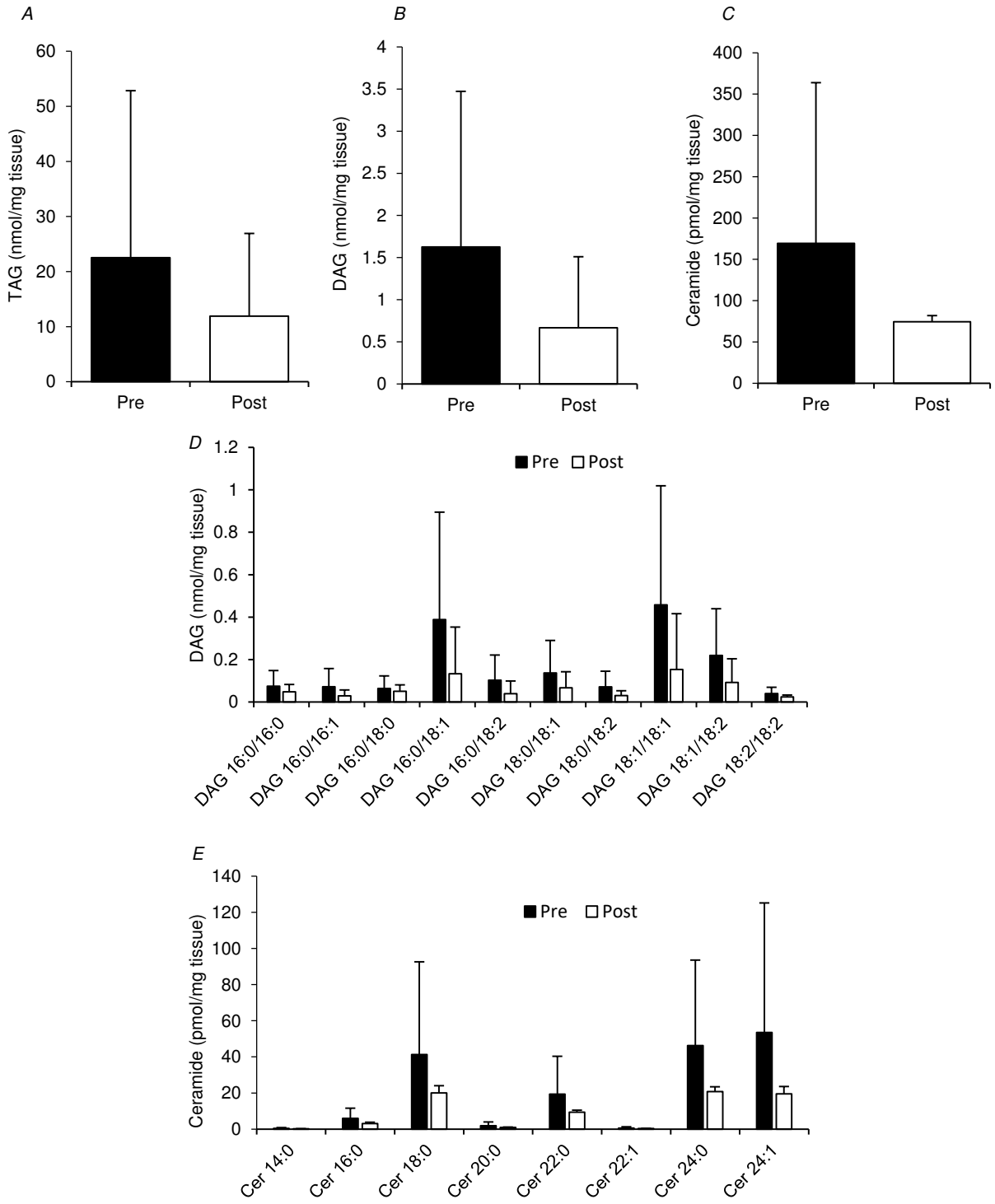
A
TAG (nmol/mg tissue)
60
50
40
30
20
10
0
Pre
Post
B
DAG (nmol/mg tissue)
4
3.5
3
2.5
2
1.5
1
0.5
0
Pre
Post
C
Ceramide (pmol/mg tissue)
400
350
300
250
200
150
100
50
0
Pre
Post
D
DAG (nmol/mg tissue)
1.2
1
0.8
0.6
0.4
0.2
0
Pre
Post
DAG 16:0/16:0
DAG 16:0/16:1
DAG 16:0/18:0
DAG 16:0/18:1
DAG 16:0/18:2
DAG 18:0/18:1
DAG 18:0/18:2
DAG 18:1/18:1
DAG 18:1/18:2
DAG 18:2/18:2
E
Ceramide (pmol/mg tissue)
140
120
100
80
60
40
20
0
Pre
Post
Cer 14:0
Cer 16:0
Cer 18:0
Cer 20:0
Cer 22:0
Cer 22:1
Cer 24:0
Cer 24:1

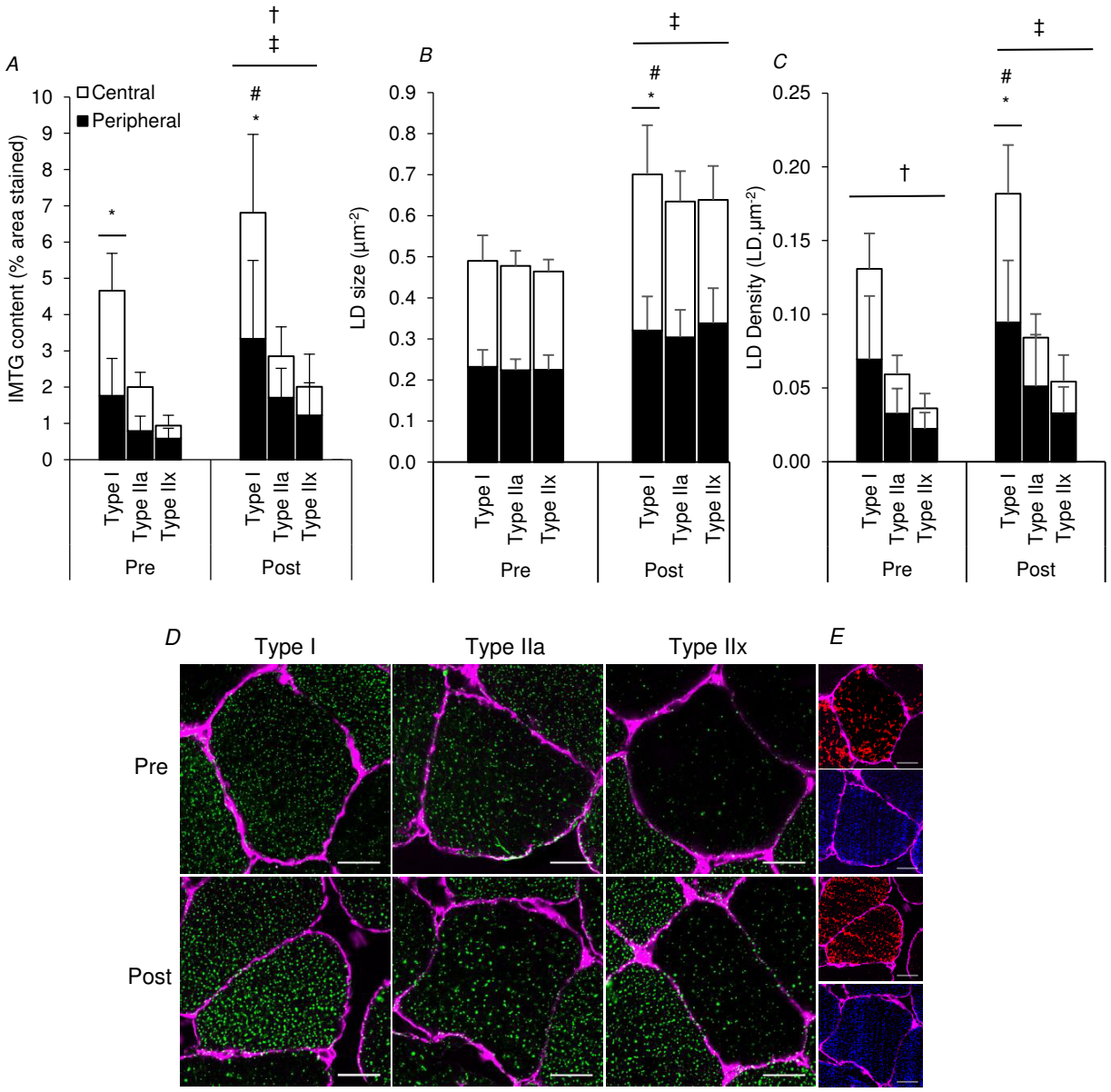
A
B
C
D
E
Central
Peripheral
IMTG content (% area stained)
LD size (µm-2)
LD Density (LD.µm-2)
Type I
Type IIa
Type IIx
Pre
Post
Type I
Type IIa
Type IIx
Pre
Post

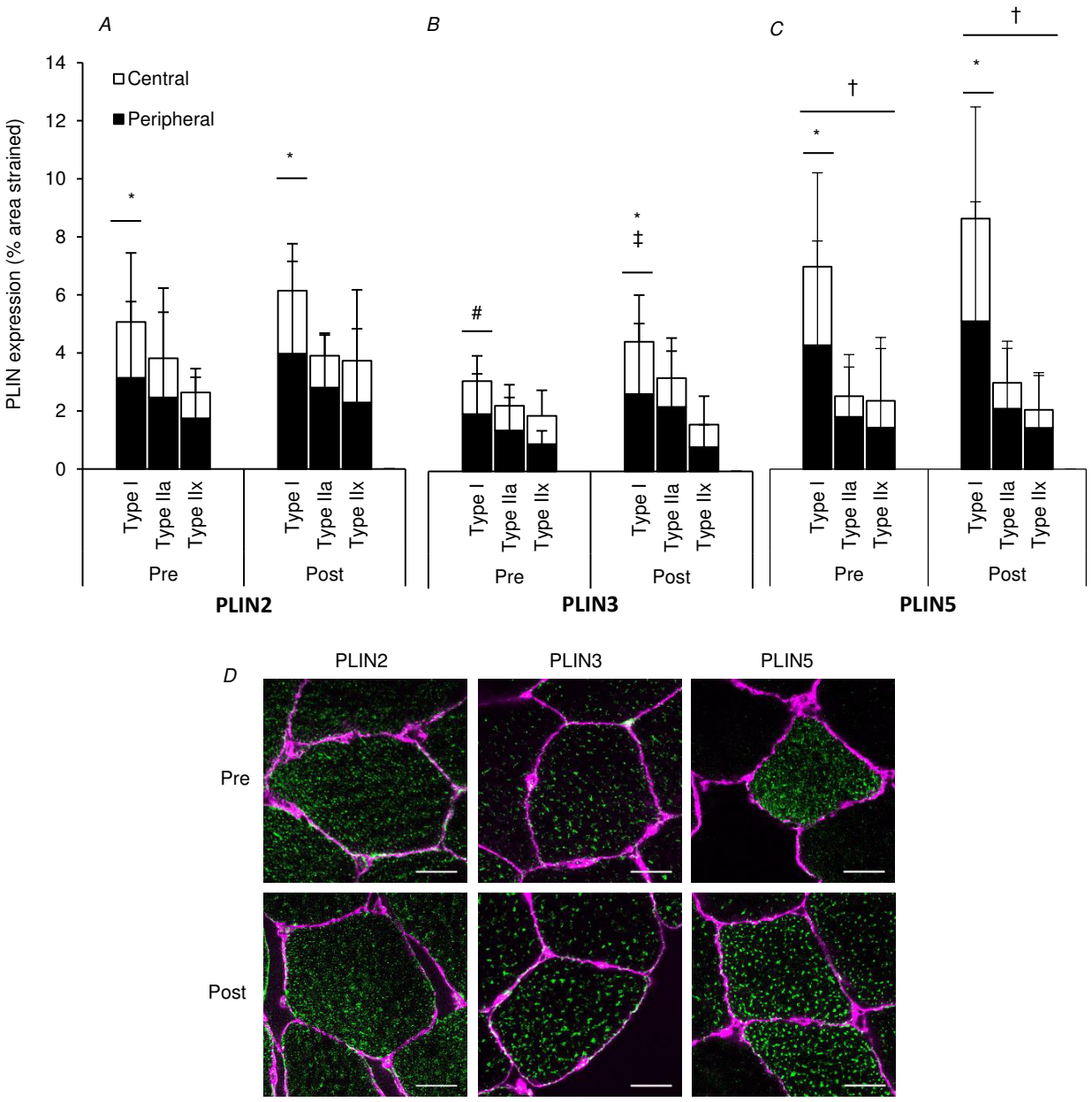
A
B
C
Central
Peripheral
PLIN expression (% area strained)
14
12
10
8
6
4
2
0
Type I
Type IIa
Type IIx
Pre
Post
PLIN2
PLIN3
PLIN5
*
#
‡
†
D
PLIN2
PLIN3
PLIN5
Pre
Post

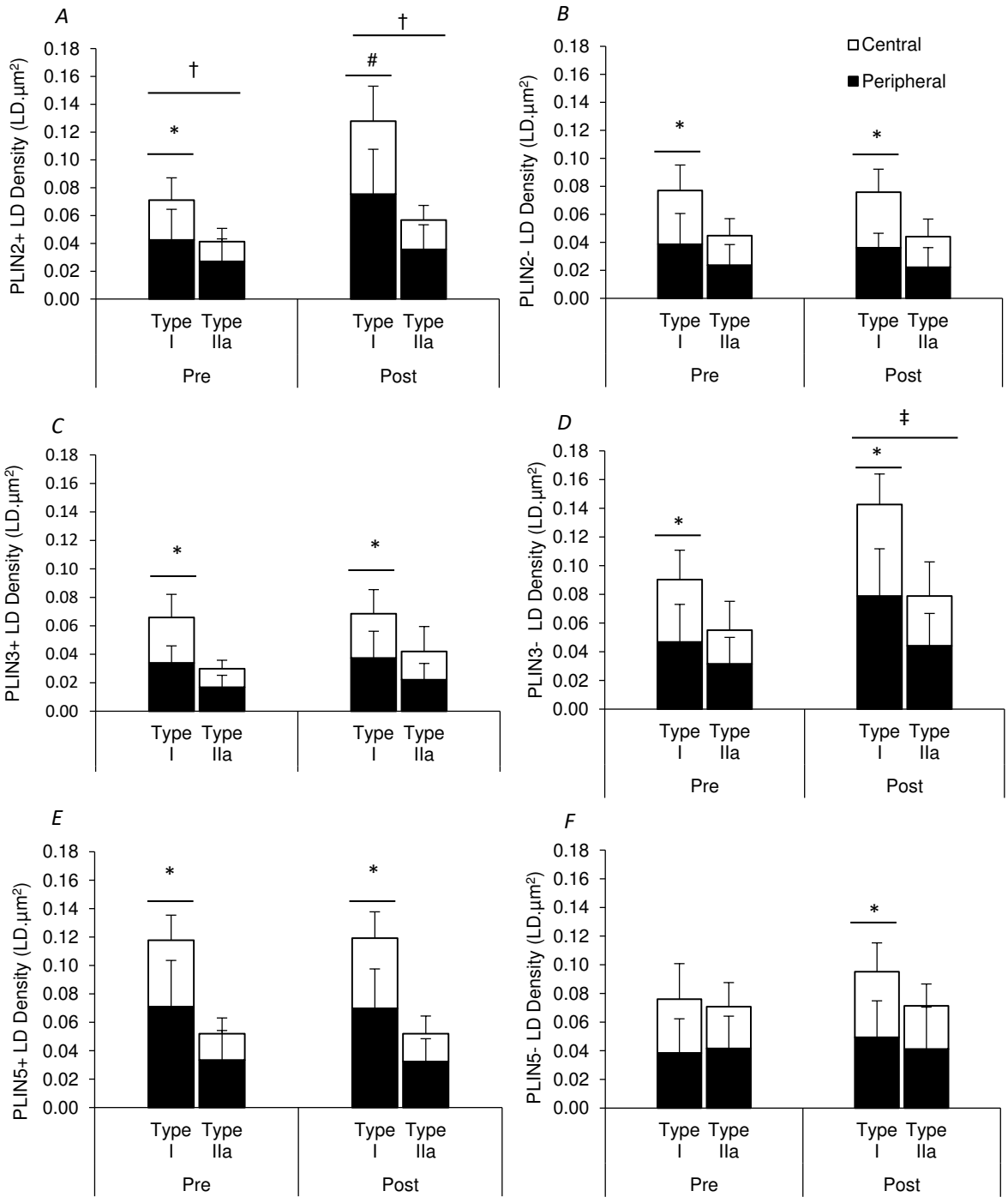
A
B
C
D
E
F
PLIN2+ LD Density (LD.µm²)
PLIN2- LD Density (LD.µm²)
PLIN3+ LD Density (LD.µm²)
PLIN3- LD Density (LD.µm²)
PLIN5+ LD Density (LD.µm²)
PLIN5- LD Density (LD.µm²)
0.18
0.16
0.14
0.12
0.10
0.08
0.06
0.04
0.02
0.00
Central
Peripheral
Type I
Type IIa
Pre
Post
*
†
‡
#